Journal of Nuclear and Radiochemical Sciences, Vol. 3, No. 2, pp. A1-A9, 2002

Accounts

Thermal and Optical Switching of Iron(III) Complexes

Shinya Hayami,*[,a] Osamu Sato,[b] Katsuya Inoue,[c] Yasuaki Einaga,[d] and Yonezo Maeda[a]

[a]*Department of Chemistry, Faculty of Sciences, Kyushu University, 6-10-1 Hakozaki, Higashi-ku, Fukuoka 812-8581, Japan*

[b]*Kanagawa Academy of Science and Technology, KSP Bldg. East 412, 3-2-1 Sakado, Takatsu-ku, Kawasaki 213-0012, Japan*

[c]*Institute for Molecular Science, Myodaiji, Okazaki 444-8585, Japan*

[d]*Department of Chemistry, Faculty of Science and Technology, Keio University, 3-14-1 Hiyoshi, Yokohama 223-8522, Japan*

Received: October 18, 2002; In Final Form: December 3, 2002

Binuclear iron(III) spin-crossover complexes, $[Fe_2(salten)_2(az)](BPh_4)_2$ (**1**) and $[Fe_2(salten)_2(cc)](BPh_4)_2$ (**2**) (H_2salten = 2,2'-[iminobis(3,1-propanediylnitrilomethylidyne)]bis-phenol, az = 4,4'-azobis-pyridine, and cc = 4,4'-(1,2-ethenediyl)bis-pyridine), and mononuclear iron(III) spin-crossover complexes, $[Fe(pap)_2]ClO_4 \cdot H_2O$ (**3**) (Hpap = 2-(2-pyridylmethyleneamino)phenol) and $[Fe(qsal)_2]NCSe \cdot CH_2Cl_2$ (**4**) (Hqsal = 2-[(8-quinolinylimino)methyl]-phenol), were synthesized and characterized by single-crystal X-ray diffraction, Mössbauer spectra, magnetic susceptibilities, and electronic spectra. The structures of **1** and **2** were determined in the low-spin state, at 100 K and the high-spin states at 298 K. The complexes **1** and **2** exhibited the spin-crossover behavior; gradual and rapid spin interconversion was observed by means of Mössbauer spectroscopy at 293 K. The structure of **3** in the high-spin state was determined at 293 K. The complex **3** exhibited the abrupt spin transition with thermal hysteresis ($T_{1/2}\uparrow$ = 180 K and $T_{1/2}\downarrow$ = 165 K). The time dependence of the magnetism and the frozen-in effect were observed for the complex **3**. Furthermore, light-induced excited spin state trapping effect was observed for the first time for iron(III) complexes. The structure of **4** in the low-spin state was determined at 200 K. The complex **4** exhibited a wide thermal hysteresis loop of 180 K ($T_{1/2}\uparrow$ = 392 K and $T_{1/2}\downarrow$ = 212 K) in the first cycle, although the hysteresis loop observed for the first cycle is apparent ones. Following the first loop, it shows a two-step spin transition in warming mode ($T_{1/2}$(S1)$\uparrow$ = 215 K and $T_{1/2}$(S2)$\uparrow$ = 282 K) and a one-step spin transition in cooling mode ($T_{1/2}\downarrow$ = 212 K).

Introduction

The first transition metal complexes with d^4, d^5, d^6, and d^7 electron configurations are usually classified into two categories according to the strength of ligand field against the mean spin-pairing energy, i.e., high-spin (HS) and low-spin (LS) complexes. Iron(III) ions are transition metal ions with five d electrons. When an iron(III) is coordinated by six donor atoms of ligands, the complex forms an octahedral conformation. The octahedral ligand field splits according to the Tanabe-Sugano diagram.[1] If the ligand field strength is comparable to the mean spin-pairing energy, the complexes exhibit a spin-crossover (SC) behavior between HS ($^6A_1$) and LS ($^2T_2$) states by external perturbations (temperature, pressure, or light). Since Cambi first observed the SC phenomenon for tris(dithiocarbamato)iron(III) complexes as the spin isomers in 1931,[2] the phenomenon has been found very often in complexes of iron(II),[3] iron(III),[4] and cobalt(II).[5] The spin transition curves of the SC behaviors exist in the various forms in solids because of long-range cooperative interactions. In particular, a number of spin-crossover iron(II) and iron(III) complexes have been studied because of the validity of Mössbauer spectroscopy.[3, 4, 6]

Recently, there has been a great interest in developing novel molecular compounds whose physical properties can be controlled by illumination.[7–12] In 1984, Decurtins et al. observed a light-induced LS $\rightarrow$ HS transition, during which the molecules can be quantitatively trapped in the excited HS state at sufficiently low temperatures (T < 50 K).[13] The phenomenon is called light-induced excited spin state trapping (LIESST), the existence of the light-induced HS state for the iron(II) SC complexes was verified with optical, Mössbauer, and magnetic susceptibility measurements.[14–21] The discovery of this LIESST effect suggested that SC complexes could be used as optical switches. In the meantime a number of iron(II) complexes with light-induced long-live metastable HS states at low temperatures have been found. The difference in metal-ligand bond length Δr^o_{HL} and the zero-point energy difference ΔE^o_{HL} between the two spin states for iron(III) SC complexes are smaller than those of iron(II) complexes, and therefore the lifetime of the light-induced HS state in the iron(III) SC complexes is very short even at 5 K.[18]

Furthermore, ligand-driven light-induced spin changes (LD-LISC) in the iron(II) SC complexes have been reported by Zarembowitch et al.[22] The spin transition of LD-LISC is classified in a new category, which consists in varying the ligand field strength through photochemical *cis-trans* isomerization of the ligand. The phenomenon has been observed by using 4-styrylpyridine derivatives at relatively high temperature as 140 K.

However, the number of the optically switchable molecular solids reported until now has been quite small. This is a reason why the strategy to achieve photo-induced switching in a solid state system has not been clarified yet. One of the requisites of optically switchable compounds is that they have nearly degenerate electronic states. Furthermore, it is known that the structural change accompanied with the switching phenomena should not be too large, because steric effects often prevent the photochemical transformation. For example, the azobenzene

*Corresponding author. E-mail: hayascc@mbox.nc.kyushu-u.ac.jp. FAX: +81-92-642-2607.

Published on Web 12/28/2002

derivatives, which are representative photochromic molecules, do not undergo *trans-cis* photo-isomerization in solid state due to the steric hindrance. This means that compounds with nearly degenerate electronic states and with only small structural changes between the metastable state and the stable state are appropriate as the materials of optical switching. However, even if these requirements are satisfied, most of the compounds never show photo-induced switching behavior with long-lived metastable states. Although it is possible to produce a metastable state using such compounds by illumination, the metastable state rapidly relaxes back to the stable state through tunneling effects due to the small structural change. Some examples were observed in iron(III) SC complexes.[23–26] The excitation of a ligand-to-metal charge transfer (LMCT) band induces the spin transition from LS to HS states. However, the photo-induced iron(III) HS states rapidly revert to the original LS states through tunneling even at 5 K, because the relaxation probability from the metastable to the stable states by tunneling increases abruptly with decrease in structural change. Hence, in order to develop a variety of optically switchable molecular solids, strategies to prevent rapid relaxation from a metastable state to a ground state should be developed. We propose the introduction of strong intermolecular interactions in molecular compounds. It is thought that the cooperativity resulting from the intermolecular interaction operates to increase the activation energy for the relaxation processes, enabling the observation of a long-lived metastable state produced by illumination as is well-known for iron(II) spin-crossover system such as $[Fe(ptz)_6](BF_4)_2$.[16, 17] That is, when the metastable molecular orientation reverts to the stable one, a large stress field might be built up in the compounds because of the presence of a strong binding energy between molecules. Hence, even if the structural change is small, the relaxation through tunneling will be substantially prevented.

In this paper, we describe our recent approaches for thermal and optical switching iron(III) complexes. We have prepared iron(III) SC complexes of which the structural change between HS and LS states is small and reported about binuclear iron(III) SC complexes **1** and **2** with photoisomerization ligands (Chart 1) and the mononuclear iron(III) complexes **3** and **4** (Chart 2) exhibiting LIESST effect and large thermal hysteresis.

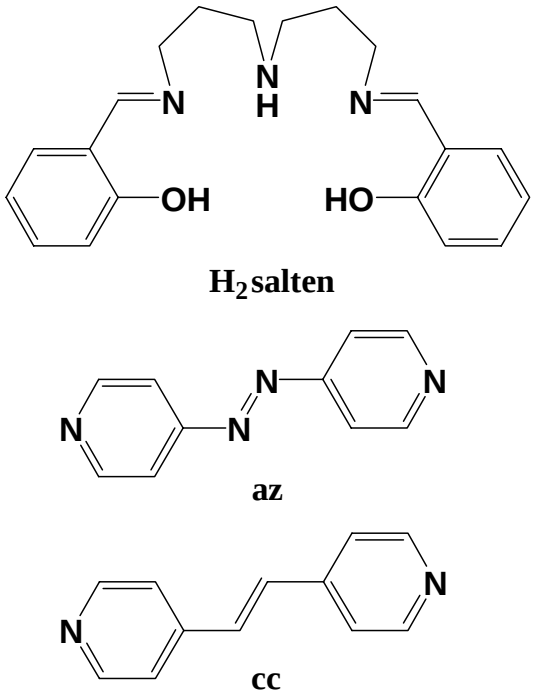

Chart 1. Structure of the ligands for H_2salten, az, and cc. H_2salten is pentadentate, and az and cc are bidentate ligands.

Results and Discussion

Iron(III) Spin-Crossover Compounds with Photo-Isomerization Ligands. The crystal structures of **1** and **2** were determined by X-ray diffraction at both 298 and 100 K.[27, 28] The space groups ($P2_1/c$ for **1** and $P2_1/a$ for **2**) are retained for both of the HS and LS states (Table 1). Each iron atom is surrounded by a nitrogen atom of pyridine and by two oxygen atoms and three nitrogen atoms of a pentadentate salten ligand.

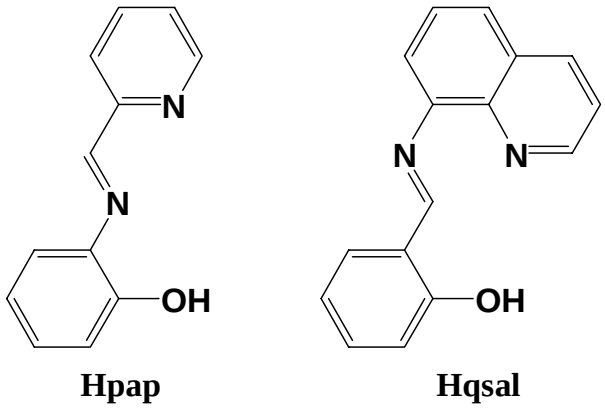

Chart 2. Structure of the ligands for Hpap and Hqsal. Hpap and Hqsal are tridentate ligands.

TABLE 1: Crystallographic Data for 1 – 4

Complex	1	2	3	4
Empirical formula	$C_{98}H_{94}O_4N_{10}B_2Fe_2$	$C_{100}H_{96}O_4N_8B_2Fe_2$	$C_{24}H_{20}O_7N_4Cl_1Fe_1$	$C_{34}H_{24}O_2N_5Se_1Cl_2Fe_1$
Formula weight	1609.20	1607.22	567.74	740.31
Crystal dimension / mm	$0.20 \times 0.30 \times 0.10$	$0.20 \times 0.20 \times 0.10$	$0.30 \times 0.30 \times 0.03$	$0.40 \times 0.40 \times 0.03$
Crystal system	monoclinic	monoclinic	triclinic	triclinic
Space group	$P2_1/_c$ (#14)	$P2_1/_a$ (#14)	$P\bar{1}$ (#2)	$P\bar{1}$ (#2)
a / Å	16.422(7)	16.554(8)	10.947(6)	11.3501(2)
b / Å	16.005(6)	15.877(3)	11.741(6)	13.9252(5)
c / Å	16.565(8)	16.823(3)	10.054(5)	10.127(1)
α / °			107.12(3)	98.327(6)
β / °	108.47(3)	109.20(2)	91.96(1)	107.055(4)
γ / °			80.51(3)	91.896(2)
V / Å^3	4129(2)	4175(1)	1217(1)	1509.3(2)
Z	2	2	2	2
D_{calcd} / gcm^{-3}	1.294	1.278	1.548	1.629
μ(MoK_α) / cm^{-1}	4.11	4.06	7.81	19.24
$R1$	0.075	0.051	0.075	0.047

The bond lengths and angles of the compounds corresponding to the spin equilibrium state at 298 K and those of the LS state at 100 K are listed in Table 2. All of the cell parameters, *a*, *b*, and *c*, for **1** and **2** decrease with increasing in temperature and the volumes of the unit cell at 298 K decrease 4.15% and 2.66% than those at 100 K for **1** and **2**, respectively.

The ORTEP views of the complexes **1** and **2** at 100 K are shown in Figures 1 and 2, respectively. The binuclear iron(III) complex **1** in which trans-form azobis(4-pyridine) (az) acts as a bridging ligand is centro-symmetric; the diazo moiety sits on the center of symmetry. The moiety of diazo (N=N) of the cation of **1** sits on a center of symmetry and two nitrogen atoms of the diazo moiety (N(5) and N'(5)) are in a *trans* geometry. The iron atom of the binuclear complex is in a pseudo-octahedral coordination with a *trans* geometry for the two salicylideneiminato moieties (N(1) and N(3)), in which the basal plane are composed of the N_2O_2 donors of these two moieties and the two axial positions are occupied by the nitrogen atom of the 3,3'-diaminodipropylamine moiety and by the nitrogen atom of az. The basal plane defined by Fe, O(1), O(2), N(1), and N(3) has a slight tetrahedral distortion: two oxygen atoms (O(1) and (O(2)) being in *trans* geometry to each other, imino nitrogen atoms (N(1) and N(3)) being in *trans* geometry, and amino and pyridine nitrogen atoms (N(2) and N(4)) being in *trans* geometry. The mean bond distances for Fe-O (1.89 Å) and Fe-N (2.03 Å) at 298 K are intermediate between the typical values of the bond distances for HS complexes, Fe-O (1.91 Å) and Fe-N (2.16 Å), and those for LS complexes, Fe-O (1.88 Å) and Fe-N (1.98 Å), at room temperature.

The structure of **2** is similar to that of **1** and is the binuclear iron(III) complex bridged by 4,4'-(1,2-ethenediyl)bis-pyridine (cc). The vinylene group is in *trans* geometry (C(26) and C'(26)), too. The values of the bond distances of Fe-O (1.89 Å) and Fe-N (2.02 Å) are intermediate between the typical values of the bond distances for HS and those for LS complexes, too.

TABLE 2: Representative Bond Distances and Angles for the Complexes 1 and 2

Complex	**1**		**2**	
	T = 298 K	*T* = 100 K	*T* = 298 K	*T* = 100 K
	Bond Distances / Å			
Fe(1)-O(1)	1.893(8)	1.866(4)	1.886(5)	1.867(5)
Fe(1)-O(2)	1.890(9)	1.881(4)	1.892(5)	1.889(5)
Fe(1)-N(1)	2.05(1)	1.963(5)	1.989(6)	1.975(6)
Fe(1)-N(2)	2.02(1)	2.000(5)	2.065(6)	2.011(6)
Fe(1)-N(3)	2.01(1)	1.944(5)	2.000(6)	1.952(6)
Fe(1)-N(4)	2.037(10)	1.988(4)	2.045(6)	2.006(6)
	Bond angles / º			
O(1)-Fe(1)-O(2)	176.9(4)	177.8(2)	177.7(3)	179.4(2)
O(1)-Fe(1)-N(1)	89.1(5)	88.9(2)	90.6(2)	89.8(3)
O(1)-Fe(1)-N(2)	91.9(4)	90.9(2)	92.6(3)	89.3(2)
O(1)-Fe(1)-N(3)	89.8(4)	90.1(2)	89.9(2)	90.0(2)
O(1)-Fe(1)-N(4)	88.4(4)	89.4(2)	87.9(2)	90.7(2)
O(2)-Fe(1)-N(1)	89.1(5)	89.3(2)	90.3(2)	89.8(3)
O(2)-Fe(1)-N(2)	90.7(5)	90.4(2)	89.6(3)	91.2(2)
O(2)-Fe(1)-N(3)	92.2(4)	91.7(2)	89.3(2)	90.4(2)
O(2)-Fe(1)-N(4)	89.1(4)	89.3(2)	89.9(2)	88.8(2)
N(1)-Fe(1)-N(2)	87.3(6)	89.4(2)	87.3(3)	89.5(3)
N(1)-Fe(1)-N(3)	172.8(6)	177.0(2)	175.8(3)	178.1(3)
N(1)-Fe(1)-N(4)	94.6(6)	91.3(2)	92.3(3)	90.8(3)
N(2)-Fe(1)-N(3)	85.6(6)	87.7(2)	88.6(3)	88.6(3)
N(2)-Fe(1)-N(4)	178.0(5)	179.2(2)	179.3(2)	179.7(3)
N(3)-Fe(1)-N(4)	92.5(5)	91.6(2)	91.8(3)	91.1(3)

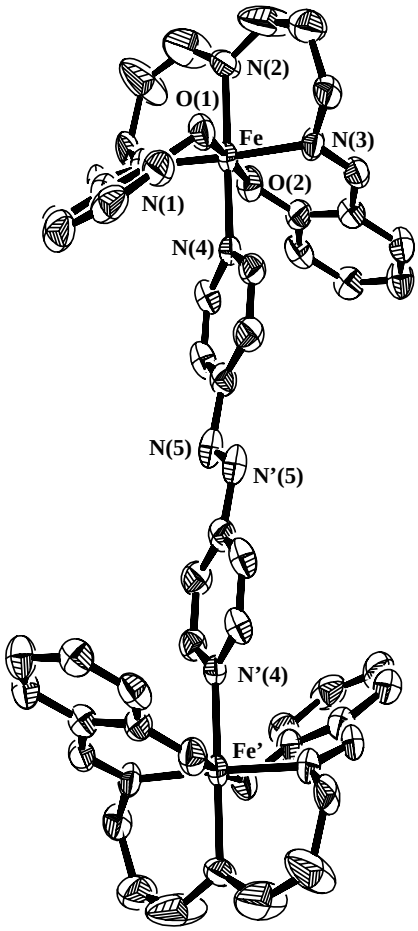

Figure 1. ORTEP view of $[Fe_2(salten)_2(az)]^{2+}$ ($\mathbf{1}^{2+}$) at 100 K showing 50% probability displacement ellipsoids. All hydrogen atoms are omitted for clarity.

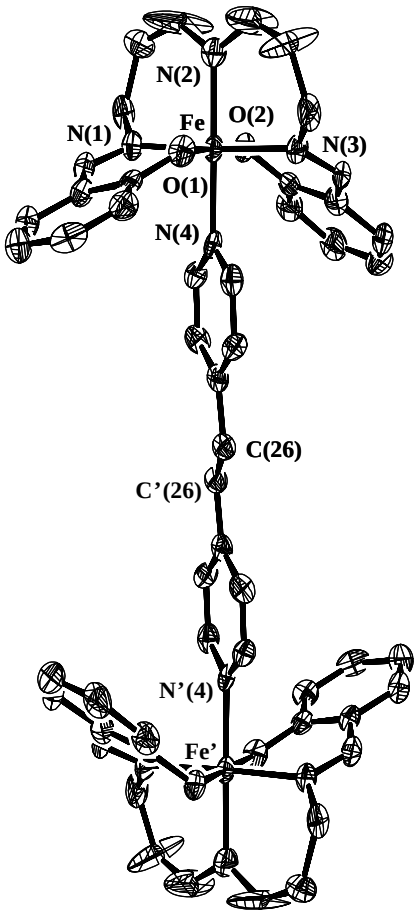

Figure 2. ORTEP view of $[Fe_2(salten)_2(cc)]^{2+}$ ($\mathbf{2}^{2+}$) at 100 K showing 50% probability displacement ellipsoids. All hydrogen atoms are omitted for clarity.

At 100 K, the arrangements of **1** and **2** units are quite similar to those at 298 K. The values of the mean bond distances of Fe-O (1.87 Å) and Fe-N (1.97 Å) are the typical values of the bond distances for LS compounds. The spin transition principally affects the FeN_4O_2 core geometry. The Fe-O bonds in LS form are 0.013 Å shorter than those for **1** at 298 K and the Fe-N bonds in LS form are 0.056 Å shorter than those for **1** at 298 K. The structure of **2** at 100 K is similar to that of **2** at 298 K. The values for the mean bond distances of Fe-O (1.88 Å) and Fe-N (1.99 Å) are intermediate between the typical values of the bond distances for LS compounds. The Fe-O bonds in LS form are 0.011 Å shorter than those for **2** at 298 K and the Fe-N bonds are 0.039 Å shorter than those for **2** at 298 K. It should be noted that a slight conformational change of the chelate rings makes the tetrahedral distortion of the FeO_2N_2 basal plane and change in the iron-coordination atom bond lengths, and as a result it induces the spin transition.

The temperature dependencies of magnetic susceptibilities were measured in the temperature range of 1.8 K to 350 K and $\chi_m T$ vs. T plots for **1** and **2** are shown in Figure 3. The values of $\chi_m T$ for **1** and **2** are constant (0.5 cm^3 K mol^{-1}) in the temperature range of 1.8 - 200 K, and the values are those observed for LS complexes. The $\chi_m T$ values increase gradually from 0.5 cm^3 K mol^{-1} at 200 K to ca 2.5 cm^3 K mol^{-1} for **1** and to 1.9 cm^3 K mol^{-1} for **2** at 350 K. The magnetic behavior for the increasing and decreasing temperature sequences is practically similar to each other, and the spin transition between HS and LS states is not associated with a thermal hysteresis. The results suggest that **1** and **2** are classified as a continuous type of the spin transition.[18] The value of the magnetic moment of **1** at 350 K is larger than that of **2**, i.e. the ligand field strength of **2** with cc (vinyl group) is stonger than that of **1** with az (azo group). The value of 0.5 cm^3 K mol^{-1} is characteristic of an iron(III) complex in a LS state; a value of 0.38 cm^3 K mol^{-1} (spin-only value) would be expected for iron(III) complexes in a LS state. Clearly the complexes **1** and **2** are in the LS state (S = 1/2) below 200 K. The values of $\chi_m T$ for **1** and **2** at 350 K are smaller than the typial values for HS (S = 5/2) compounds. There are two possibilities for the small $\chi_m T$ values at 350 K, i.e., the small values suggest that the complexes are the mixtures of HS and LS species (S = 1/2 and S = 5/2) or that the complexes show rapid spin-equilibrium behavior (S = 1/2 $\leftrightarrow$ S = 5/2).

The variable temperature Mössbauer spectra of **1** and **2** are shown in Figures 4 and 5, respectively. The typical absorption for low-spin iron(III) with a large quadrupole of *Q.S.* = 1.65 mm s^{-1} doublet and an isomer shift of *I.S.* = 0.29 mm s^{-1} is observed in the spectrum of **1** at 80 K. The spin state expected from the spectrum is agreed with that obtained from the magnetic measurements. The *Q.S.* of **1** at 95 K, 1.65 mm s^{-1}, is less than that of the iron(III) complexes with salten ligand reported previously (2.72 mm s^{-1});[29] the decrease seems to result from the change in the electric field gradient due to lattice contribution because the iron atoms have a distorted octahedral coordination. On the other hand, the spectrum of **1** at 298 K shows a small doublet (*Q.S.* = 0.886 mm s^{-1}) with *I.S.* = 0.28 mm s^{-1}. The spin state expected from the Mössbauer parameters and the values of $\chi_m T$ suggests the rapid spin

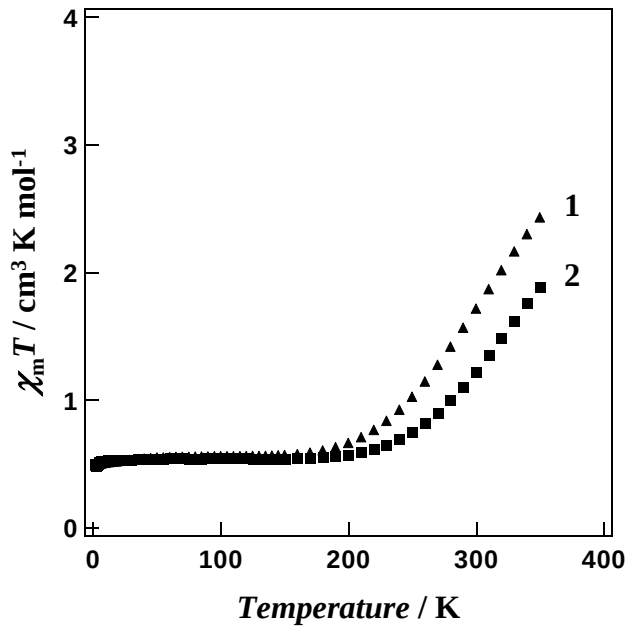

Figure 3. $\chi_m T$ versus T plots for **1** (▲) and **2** (■). Sample was warmed from 5 K to 350 K at a rate of 2 K min^{-1}.

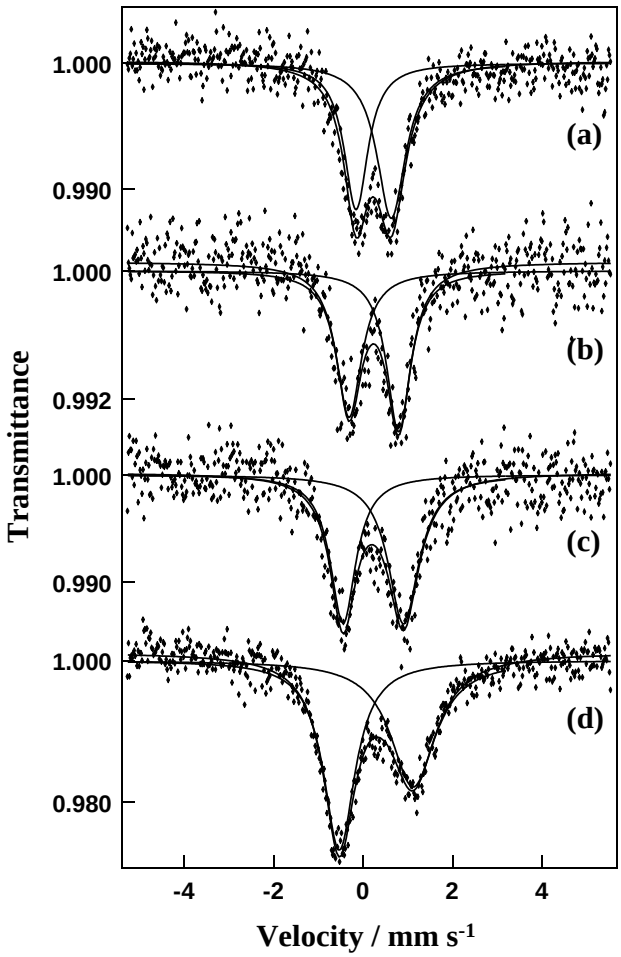

Figure 4. Mössbauer spectra of **1** (a) at 298 K, (b) at 200 K, (c) at 100 K, and (d) at 80 K.

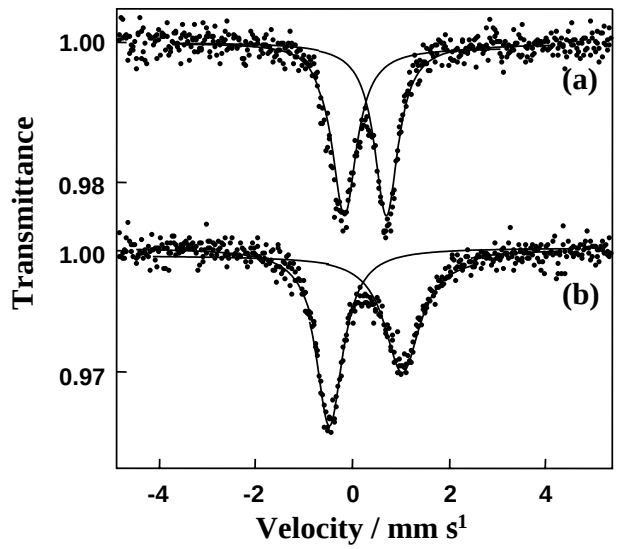

Figure 5. Mössbauer spectra of **2** (a) at 298 K and (b) at 80 K.

conversion between HS and LS states. The spectra for rapid spin interconversion between HS and LS states have been theoretically calculated by Maeda et al.[30] It is expected that the relaxation spectra with the end components (the spectra for HS or LS species) of an antisymmetric doublet are not reliably analyzed, and the spin interconversion rate for **1** could not be calculated from the spectra. However, it is expected that the spin interconversion rate between HS and LS states for **1** is faster than the inverse of the lifetime of the excited Mössbauer nuclear state (107 s^{-1}) at 298 K. The values of the bond distances of Fe-O (1.89 Å) and Fe-N (2.03 Å) are intermediate between the typical values of the bond distances for HS and those for LS complexes. The Mössbauer spectra of **2** are similar to those of **1**; the spectra are composed of a large doublet (*Q.S.* = 1.53 mm s^{-1}) at 80 K have a small doublet (*Q.S.* = 0.94 mm s^{-1}) at 298 K. The spin state at 298 K estimated from the Mössbauer parameters (*I.S.* = 0.19 mm s^{-1}) and the values of $\chi_m T$ shows the rapid spin-equilibrium between HS and LS states.

The temperature dependence of the electronic spectra was measured in acetonitrile. The binuclear complexes **1** and **2** showed thermochromic behavior. Figure 6 shows the temperature dependence of the spectra for **1**. At 60 ºC, the spectrum of **1** exhibits absorption bands at 405 and 470 nm with extinction coefficients (ε) of 2190 and 1740 L mol^{-1} cm^{-1}, respectively attributable to ligand-to-metal charge transfer (LMCT) bands. Hauser et al. reported that the bands with the extinction coefficients on the order of 103 L mol^{-1} cm^{-1} for iron(III) compounds correspond to the LMCT transitions.[31] On lowering the temperature, the absorption at 405 nm decreases in intensity and that at 470 nm shifts to a longer wavelength. The spectral change is similar to those of the spin-crossover complexes with salten reported previously.[29] The temperature dependence of the electronic spectrum is due to the spin-equilibrium between HS and LS states. The spectral changes are associated with two isosbestic points at 365 and 490 nm. Figure 7 shows the temperature dependence of the spectra for **2**. At 60 ºC, the spectrum exhibits bands at 400 and 470 nm; the absorption at 400 nm decreases in intensity with decreasing temperature and that at 470 nm shifts to a longer wavelength accompanied by the decrease in intensity with lowering the temperature. The temperature dependence of the electronic spectra is also due to the spin-equilibrium between HS and LS states. The spectrum changes with a set of isosbestic points at 370 and 520 nm.

Iron(III) Spin Transition Compounds Exhibiting LIESST Effect. Strong intermolecular interaction can be achieved by using π–π interactions as well as by using bridging ligands.[20, 21, 32–35] The iron(III) compound we focused on is $[Fe(pap)_2]ClO_4 \cdot H_2O$ (**3**).[36, 37] The planar ligand, pap, with corresponding π electrons, has a potential ability to interact with neighboring ligands by π–π interactions. In fact, the presence of a strong intermolecular interaction is suggested from the single crystal X-ray analysis. Single crystals suitable for X-ray diffraction of **3** were isolated by slow diffusion in methanolic solutions. The complex **3** crystallizes in the triclinic $P\bar{1}$ space group at room temperature (Table 1). The X-ray structure of **3** revealed that the iron(III) ion has an octahedral coordination with an N_4O_2 donor set (Figure 8(a)). Its electronic state is hence situated just in the critical region between high-spin and low-spin states, i.e., nearly degenerate. The bond lengths of Fe-O(1), Fe-O(2), Fe-N(1), Fe-N(2), Fe-N(3), and Fe-N(4) for **3** are 1.93, 1.93, 2.11, 2.20, 2.14, and 2.14 Å, respectively. The values of the bond lengths are consistent with those typical for HS iron(III) compounds. Two tridentate ligands are found to be perpendicular to one another. $[Fe(pap)_2]^+$ cations form short contacts (3.50 Å) with neighboring molecules through the pyridine and phenyl rings in the ligands on an *ab* plane, providing a 2-D sheet extended by the π-π interactions (Figure 8(b)). The 2-D sheets align along *c* axis. The water molecules and perchlorate ions exist between the 2-D sheets and are hydrogen-bonded to each other. The molecular packing of **3** is very tight. This suggests that there are strong intermolecular interactions in the molecular assembly. It should be noted that the structure of complex **3** has no remarkable features at the single molecule level compared to other typical iron(III) spin-crossover complexes.

The HS to LS conversion was followed by measurement of the magnetic susceptibility (Figure 9) and Mössbauer spectra (Figure 10) as a function of temperature. At room temperature, the value of $\chi_m T$ for **3** is equal to 3.9 cm^3 K mol^{-1}. The Mössbauer spectrum for **3** at room temperature shows a small doublet (*Q.S.* = 1.11 mm s^{-1}; *I.S.* = 0.36 mm s^{-1}) which can be assigned to the HS state of iron(III). On cooling, the value of $\chi_m T$ drops abruptly around $T_{1/2}\downarrow$ = 165 K. The $\chi_m T$ value at 100 K is equal to 0.51 cm^3 K mol^{-1}. The Mössbauer spectrum at 13 K for **3** shows a large doublet (*Q.S.* = 3.08 mm s^{-1}; *I.S.* = 0.11 mm s^{-1}) which can be assigned to the LS state of iron(III). In the warming mode, an abrupt variation of $\chi_m T$ was observed around $T_{1/2}\uparrow$ = 180 K. Fairly abrupt transitions with a hysteresis loop (ca. 15 K) support the presence of the strong cooperative interaction. Another important point is that this complex exhibits a frozen-in effect[19, 37–39] which is observed for the materials with large cooperativity. If the sample is rapidly

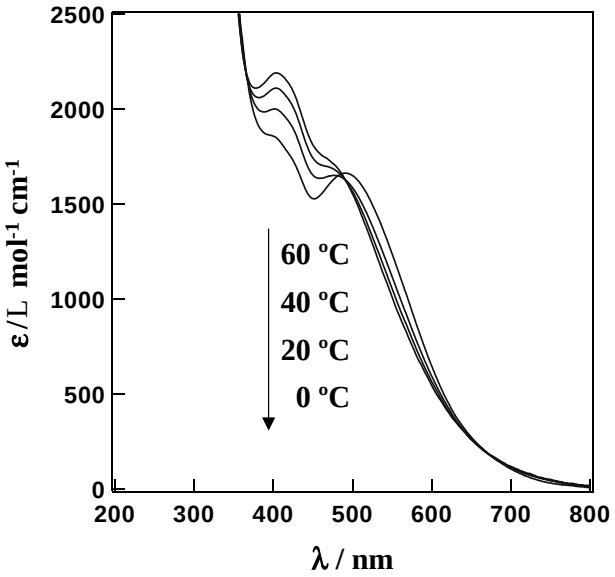

Figure 6. Temperature dependence of the electronic spectra of **1** in acetonitrile solution at the temperature range between 60 ºC - 0 ºC.

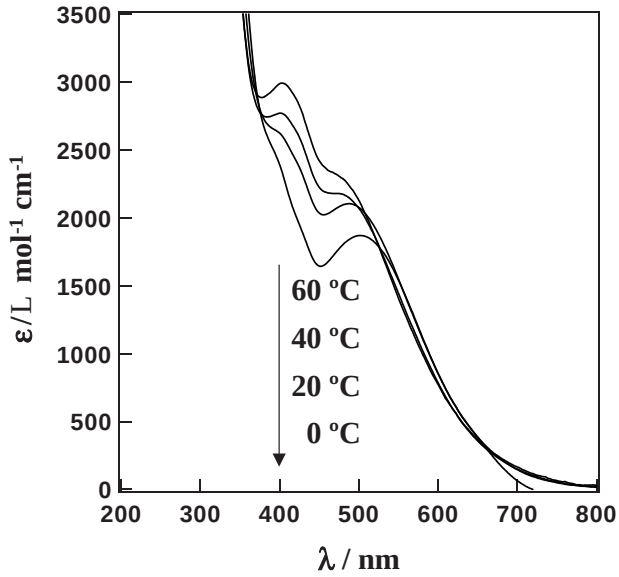

Figure 7. Temperature dependence of the electronic spectra of **2** in acetonitrile solution at the temperature range between 60 ºC - 0 ºC.

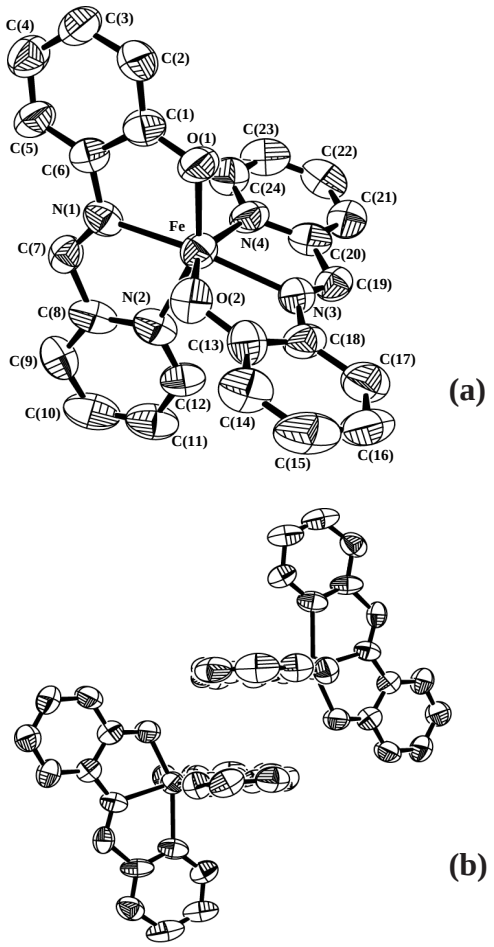

Figure 8. Molecular structures in the high-spin state at 298 K. (a) ORTEP view of $[Fe(pap)_2]^+$ (**3**$^+$) showing 50% probability displacement ellipsoids. (b) Structure of the π–π stucking between complexes. All hydrogen atoms are omitted for clarity.

quenched in liquid helium, whereby the sample temperature drops from room temperature to 4.2 K within a few seconds, the HS state may be "frozen-in" and a transition to LS state is not observed even in a few days. The relaxation rate from HS to LS is quite slow. These experimental results support that strong cooperative interactions operate in this compound.

It has been reported that a broad band (from 500 to 800 nm) in UV-vis spectrum for the LS iron(III) complex can be attributed to the spin-allowed LMCT transition.[23, 24] Furthermore, Hauser et al. reported that the excitation of the LMCT band results in the transient generation of HS iron(III) fractions.[23, 24] Hence, in order to excite the LMCT band of complex **3**, light (540 - 550 nm) passing through a combination of IR cut-off and green filters was guided via an optical fiber into a SQUID magnetometer. The sample was placed on the edge of an optical fiber. When the sample was illuminated at 5 K, the increase of the magnetization value was observed.[40] This suggests that the transition from LS to HS was induced by illumination. The change in the magnetization persisted for periods of at least ten hours after the illumination. Figure 10 shows a series of Mössbauer spectra that were recorded at 13 K before and after the excitation with light. In order to enhance the Mössbauer spectra, ^{57}Fe-enriched sample was used. The spectrum in Figure 10(b) measured before illumination at 13 K shows a large doublet (*Q.S.* = 3.08 mm s^{-1}; *I.S.* = 0.11 mm s^{-1}), representing the LS state. The spectrum measured after illumination for 15 min shows a small doublet (*Q.S.* = 1.14 mm s^{-1}, *I.S.* = 0.44 mm s^{-1}), representing the HS state. Thus, it has been confirmed that the LS state changed to the HS state by illumination. These indicate clearly that the visible light illumination of complex **3** induces the LMCT, followed by relaxation to a metastable HS state. When the

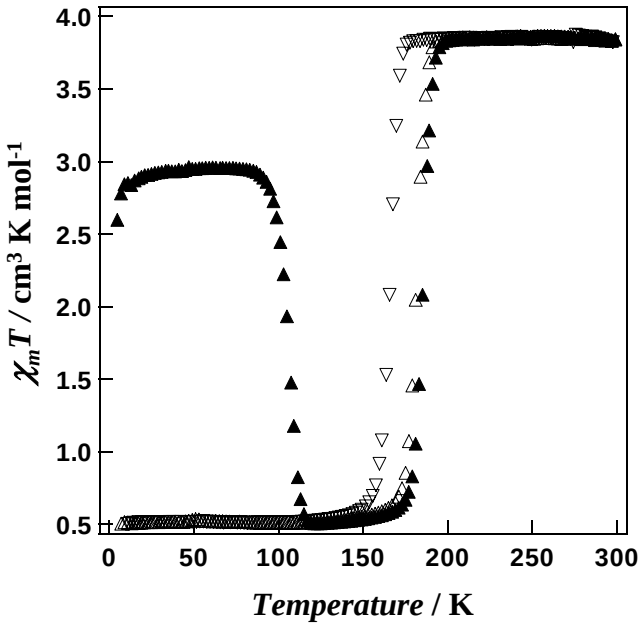

Figure 9. $\chi_m T$ versus T plots for **3**. Sample was cooled from 300 K to 5 K (▽) and then warmed from 5 K to 300 K (△) at a rate of 2 K min^{-1}. Sample was warmed at a rate of 2 K min^{-1} after it was quenched to 5 K (▲).

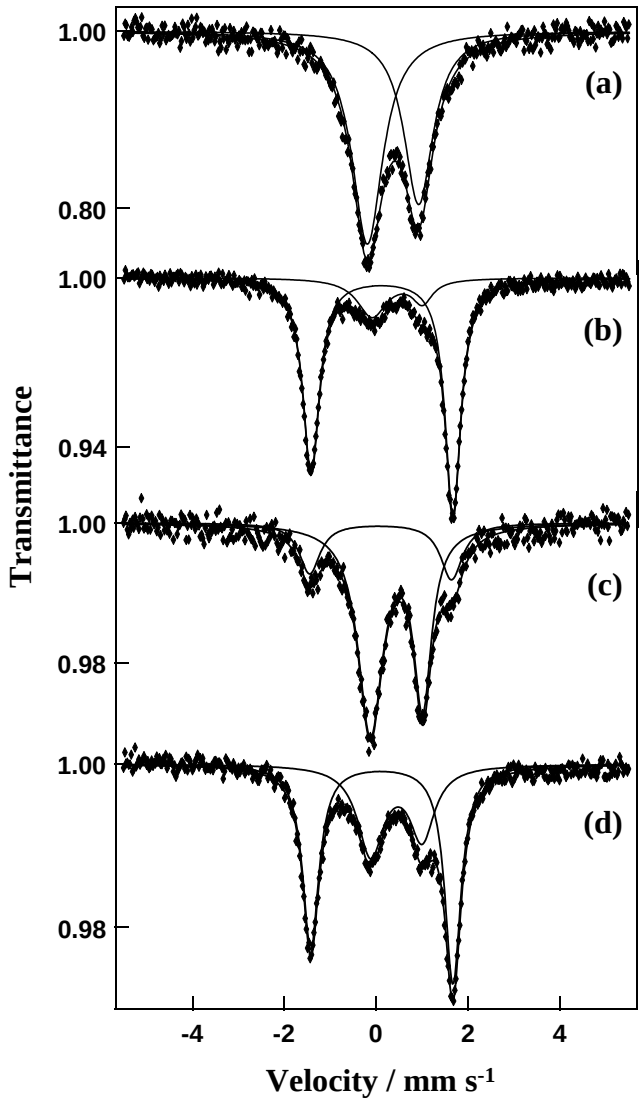

Figure 10. ^{57}Fe Mössbauer spectra for **1**. (a) Spectrum at 298 K, (b) spectrum at 13 K before illumination, (c) spectrum at 13 K after illumination and (d) spectrum at 13 K after thermal treatment at 130 K.

temperature is raised to 150 K for a few minutes and is again lowered to 13 K, the metastable state is found to have relaxed back to the LS ground state (*Q.S.* = 3.08 mm s^{-1}; *I.S.* = 0.11 mm s^{-1}). The metastable state could be maintained for a long time, provided that the sample was kept below ca. 70 K. The achievement of an anomalous long-lived metastable state is considered to be due to the presence of the strong intermolecular interaction. We believe that this approach may be valuable in developing novel optically switchable molecular compounds.

Iron(III) Spin Transition Compound with Wide Thermal Hystresis. Iron(III) complex $[Fe(qsal)_2]NCSe \cdot CH_2Cl_2$ (**4**) exists in the LS state at room temperature when they are synthesised in $MeOH/CH_2Cl_2$ solutions. X-ray analysis was successfully carried out for the compound **4** at 230 K. Figure 11 shows that when the complexe **4** is in the LS state it crystallizes in a triclinic $P\bar{1}$ space group (Table 1). The single crystal X-ray analysis of **4** reveales that the iron(III) atoms are octahedrally co-ordinated by four nitrogen atoms and two oxygen atoms of two qsal ligands, i.e., an N_4O_2 donor set. The values of the bond lengths (1.88 Å for Fe-O and 1.97 Å for Fe-N) are consistent with those for typical LS iron(III) compounds. The Fe-O distances are shorter than the Fe-N distances, which induce a pronounced distortion of the FeN_4O_2 octahedron. The qsal ligands form slightly distorted planes. The dihedral angles between the phenyl ring and Fe-O(1)-N(1) chelate ring, between the other phenyl ring and Fe-O(2)-N(3) chelate ring, between the quinoline ring and Fe-N(1)-N(2) chelate ring, and between the other quinoline ring and Fe-N(3)-N(4) chelate ring for **4** are equal to 2.43°, 9.52°, 0.68°, and 3.66°, respectively.

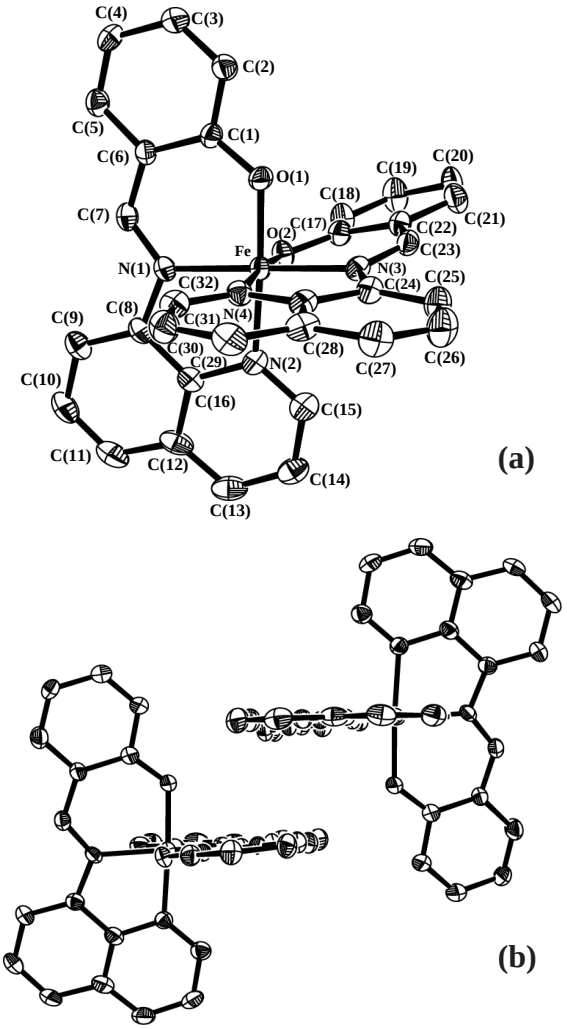

Figure 11. Molecular structures in the low-spin state at 200 K. (a) ORTEP view of $[Fe(qsal)_2]^+$ ($\mathbf{4}^+$) showing 50% probability displacement ellipsoids. (b) Structure of the π–π stucking between complexes. All hydrogen atoms and solvent molecule are omitted for clarity.

The two tridentate ligands in the complexes are found to be nearly perpendicular to one another: the least-square plane of the slightly distorted qsal ligands for **4** makes a dihedral angle of 79.49° and 80.44° with one of the other qsal ligands. No counter anion $NCSe^-$ and no solvent molecules are located in the first co-ordination sphere. The crystal structure of the solvated **4** could not be determined in the HS form because the spin transition induces cracks in the crystal, making an X-ray single crystal study impossible.

The temperature dependence of the magnetic susceptibility for the single crystal of **4** was measured at a rate of 2 K min^{-1} and the result is shown in the form of the $\chi_m T$ vs. T plot (Figure 12). The $\chi_m T$ value for **4** is equal to 0.36 cm^3 K mol^{-1} at 150 K, which is in the range of the values expected for the LS iron(III) ions. As the temperature is increased over 150 K, the $\chi_m T$ product remains constant from 150 K to 350 K, and then abruptly increases around $T_{1/2}\uparrow$ = 392 K. The $\chi_m T$ value at 400 K is 3.8 cm^3 K mol^{-1}, showing that the spin transition from the LS to the HS state is induced. The spin transition is directly related to the removal of solvent molecules. Thermogravimetry (Figure 13) carried out with the same

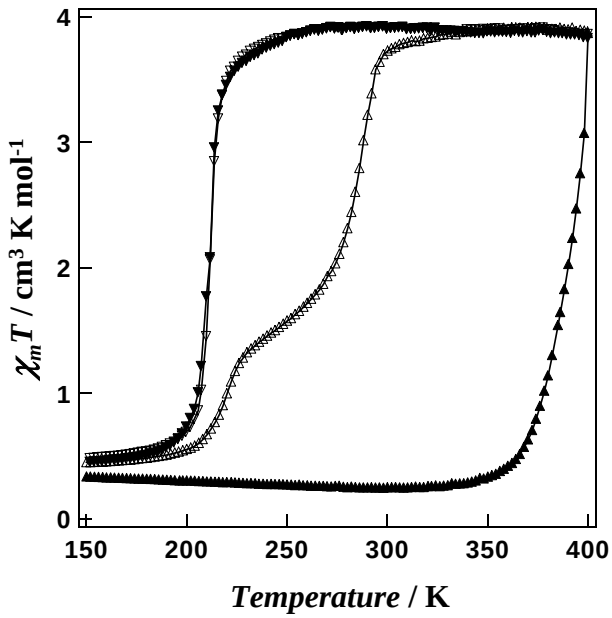

Figure 12. $\chi_m T$ versus T plots for **4**. The sample was warmed from 5 K to 400 K (▲) and cooled from 400 K to 5 K (▼) in the first cycle, and then the sample was warmed from 5 K to 400 K (△) and cooled from 400 K to 5 K (▽) in the second cycle at a rate of 2 K min^{-1}.

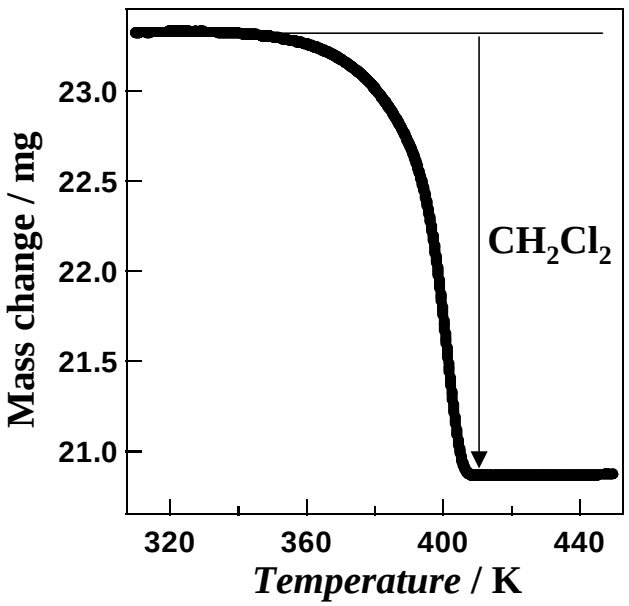

Figure 13. Thermogravimetric analysis for **4**. (2.356 mg of sample)

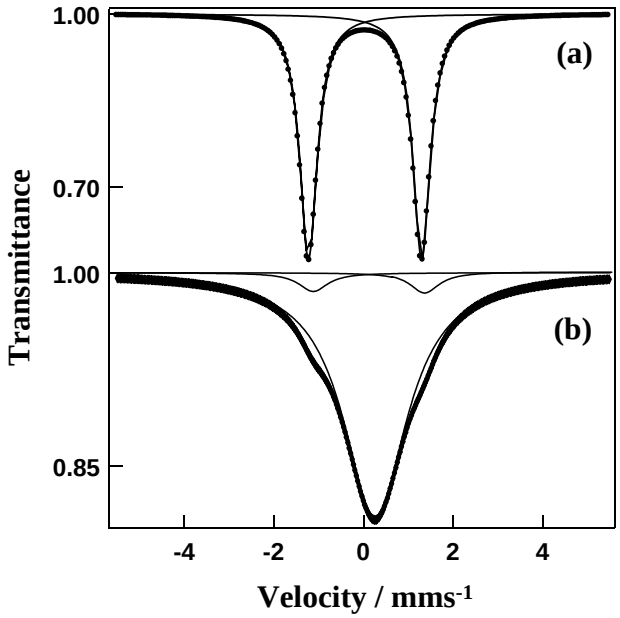

Figure 14. ^{57}Fe Mössbauer spectra at room temperature (a) before and (b) after annealing at 400 K for **4**. There is a small amount of LS form in the HS form after annealing, indicating that solvent molecules are still retained.

heating rate (2 K min^{-1}) as for the magnetic susceptibility measurements revealed a continuous loss of mass, starting at room temperature. The decrease in mass proceeds rapidly in the temperature range 380 K - 410 K. At 420 K, the mass lost is in agreement with the removal of a CH_2Cl_2 molecule. Elemental analysis also supports the desolvation. On cooling, the $\chi_m T$ value for the non-solvated compound **4** was almost constant from 400 K to 220 K, then abruptly dropped at around $T_{1/2}\downarrow$ = 212 K, showing that the HS moieties were restored to the LS state. The first hysteresis loop of 180 K ($T_{1/2}\uparrow$ = 392 K and $T_{1/2}\downarrow$ = 212 K) is an apparent one because the desolvation occurs at elevated temperature. It should be noted that a similar large apparent hysteresis has been reported for [Fe(hyetrz)$_3$](3-nitrophenylsulfonate)$_2\cdot 3H_2O$ by Garcia et al.[41, 42]

A second heating experiment revealed that the spin-crossover takes place in a two-step manner.[43–51] The so-called "step 1" and "step 2" are centred around the temperatures $T_{1/2}(S1)\uparrow$ = 215 K and $T_{1/2}(S2)\uparrow$ = 282 K, respectively. The magnetic behavior shows that the fraction of the LS to HS spin transition in the upper step "step 2" is about twice as high as that in the lower step "step 1". Additional thermal cycles did not modify the thermal hysteresis loop. The $\chi_m T$ value at the inflection point at around 250 K is 1.6 cm^3 K mol^{-1}. When the hysteresis widths (ΔT) in "step 1" and "step 2" are defined as the differences of $T_{1/2}(S1)\uparrow$ and $T_{1/2}\downarrow$ and of $T_{1/2}(S2)\uparrow$ and $T_{1/2}\downarrow$, respectively, they are estimated to be 3 K (step 1) and 70 K (step 2). In order to confirm the transition of the SC, Mössbauer spectra for **4** were measured at room temperature before and after annealing at 400 K (Figure 14). The complex was prepared with using ^{57}Fe to enhance the Mössbauer signal. Before annealing, a large doublet with *Q.S.* = 2.47 mm s^{-1} and *I.S.* = 0.11 mm s^{-1} for **4** was observed at room temperature, which corresponded to the LS state of iron(III) compounds. After being annealed at 400 K, a broad singlet (Γ_{exp} = 2.21 mm s^{-1}) with ***Q.S.*** = 0.46 mm s^{-1} and *I.S.* = 0.23 mm s^{-1} was observed at room temperature, showing that the iron(III) turns from the LS state to the HS state. This is consistent with the magnetic properties described above.

It should be noted that several examples of the two-step spin transition have been reported. Compared with these examples, the present compounds have the following important characteristics; (i) the spin transition shows a hysteresis loop, and (ii) the two-step spin crossover is observed only in the warming mode. To the best our knowledge, this kind of hysteresis behaviour has not been reported previously. Furthermore, the hysteresis width of 70 K in "step 2" is quite wide, compared with those reported elsewhere. The abrupt phase transition with the hysteresis effect suggests that a strong intermolecular interaction operates in this complex.[40]

It is useful to compare the hysteresis width of the non-solvated complexe **4** with those reported previously.[20, 21, 41–52] Several compounds with a polymeric structure have been found to display a wide thermal hysteresis. Kahn et al. reported that an iron(II) compound, [Fe(Htrz)$_{3-3x}$(4-NH$_2$trz)$_{3x}$](ClO$_4$)$_2\cdot n$H$_2$O (x = 0.05) (Htrz = 1,2,4-1H-triazole, 4-NH$_2$trz = 4-amino-1,2,4-triazole) which has a polymeric structure, displays a thermal hysteresis at the range of room temperature ($T_{1/2}\uparrow$ = 304 K and $T_{1/2}\downarrow$ = 288 K).[53, 54] However, the polymeric compound is not strictly molecular, as was concluded by previous studies.[41, 42, 53–55] Several mononuclear molecules have also exhibited thermal hysteresis loops. The maximum hysteresis width observed for iron(II) complexes with intermolecular π-π interactions is 40 K,[20, 21, 51, 52] which is narrower than that observed for the non-solvated complex **4**. Furthermore, it has been reported that the iron(II) compound, [Fe(2-pic)$_3$]Cl$_2\cdot$H$_2$O (2-pic = 2-picolylamine), exhibits the widest thermal hysteresis loop of 91 K with $T_{1/2}\uparrow$ = 295 K and $T_{1/2}\downarrow$ = 204 K.[56, 57] The structure of the compound has not been fully analysed yet. These previous results show that the hysteresis width of 70 K presented here[58] is one of the widest values among the spin-crossover complexes reported so far.[20, 21, 32–55]

In summery, we have prepared the binuclear iron(III) complexes **1** and **2** with bridging photoisomerization ligands az or cc, and the complexes **1** and **2** exhibit spin-crossover behavior depending on temperature. The Mössbauer spectra for **1** and **2** show a doublet at 293 K, suggesting the rapid spin conversion between HS and LS states. The average bond lengths of Fe-O and Fe-N for **1** and **2** are intermediate between the typical values of the bond lengths for HS and those for LS complexes. However, it is very difficult to observe *cis-trans* photoisomerization for the complexes with photoisomerization ligands in solid state. We have succeeded in observing the LIESST effect for the iron(III) complex **3** for the first time. This suggests that the cooperative interactions such as π–π interactions and hydrogen bonding can prevent the rapid relaxation from the metastable state to the stable state. It is important that our approach, the introduction of intermolecular interactions to trap the metastable state, can be widely applied not only to the design of other metal complexes with LIESST effects, but also in the design of a variety of optically switchable molecular compounds. Furthermore, we have shown that the iron(III) complex **4** displays a wide apparent hysteresis in the first cycle. After the first cycle, they show a two-step transition in the warming mode and a one-step transition in the cooling mode. The hysteresis width in "step 2" after the first cycle is 70 K, which is one of the largest hysteresis effects reported so far.

Acknowledgements. This work was supported in part by a Grant-in-Aid for Science Research on Priority Areas (417) from the Ministry of Education, Culture, Sports, Science, and Technology (MEXT) of the Japanese Government and by a Joint Research Project for Regional Intensive of Kanagawa Prefecture.

References

(1) T. M. Dunn, *Modern Coordination Chemistry*, edited by J. Lewis and R. G. Wilkins (Interscience Pub. New York, 1960), Chap. 4.
(2) L. Cambi and A. Cagnasso, Atti Accad. Naz. Lincei **13**,

809 (1931).
(3) (a) H. A. Goodwin, Coord. Chem. Rev. **18**, 293 (1976). (b) P. Gütlich, Struct. Bonding (Berlin) **44**, 83 (1981). (c) P. Gütlich and A. Hauser, Coord. Chem. Rev. **97**, 1 (1990). (d) E. König, Prog. Inorg. Chem. **35**, 527 (1987). (e) E. König, Struct. Bonding (Berlin) **76**, 51 (1991).
(4) Y. Maeda and Y. Takashima, Comments Inorg. Chem. **7**, 41 (1988).
(5) J. Zarembowitch, New J. Chem. **16**, 255 (1992).
(6) (a) E. König and G. Ritter, *Mössbauer Eff. Methodol.* edited by I. J. Gruverman, C. W. Seidel, and D. K. Dieterly (Plenum, New York, 1974), vol. 9, pp. 3-21. (b) P. Gütlich, *Chemical Mössbauer Spectroscopy*, edited by R. H. Herber (Plenum, New York, 1984), pp. 287-337. (c) P. Gütlich, R. Link, and A. X. Trautwein, *Mössbauer Spectroscopy and Transition Metal Chemistry* (Springer, Berlin, 1978).
(7) O. Sato, T. Iyoda, A. Fujishima, and K. Hashimoto, Science **272**, 704 (1996).
(8) Z.-Z. Gu, O. Sato, T. Iyoda, K. Hashimoto, and A. Fujishima, J. Phys. Chem. **100**, 18289 (1996).
(9) V. I. Kudinov, A. I. Kirilyuk, and N. M. Kreines, Phys. Lett. A **151**, 358-364 (1990).
(10) G. Nieva, Phys. Rev. B **46**, 14249 (1992).
(11) D. V. Fomitchev, K. A. Bagley, and P. Coppens, J. Am. Chem. Soc. **122**, 532 (2000).
(12) Y. Teki, S. Miyamoto, K. Iimura, M. Nakatsuji, and Y. Miura, J. Am. Chem. Soc. **122**, 984 (2000).
(13) S. Decurtins, P. Gütlich, C. P. Köhler, H. Spiering, and A. Hauser, Chem. Phys. Lett. **105**, 1 (1984).
(14) S. Decurtins, P. Gütlich, K. M. Hasselbach, A. Hauser, and H. Spiering, Inorg. Chem. **24**, 2174 (1985).
(15) A. Hauser, Chem. Phys. Lett. **124**, 543 (1986).
(16) A. Hauser, J. Chem. Phys. **94**, 2741 (1991).
(17) A. Hauser, A. Vef, and P. Adler, J. Chem. Phys. **95**, 8710 (1991).
(18) P. Gütlich, A. Hauser, and H. Spiering, Angew. Chem. Int. Ed. Engl. **33**, 2024 (1994).
(19) Th. Buchen, P. Gütlich, and H. A. Goodwin, Inorg. Chem. **33**, 4573 (1994).
(20) J.-F. Létard, P. Guionneau, L. Rabardel, J. A. K. Howard, A. E. Goeta, D. Chasseau, and O. Kahn, Inorg. Chem. **37**, 4432 (1998).
(21) J.-F. Létard, J. A. Real, N. Moliner, A. B. Gaspar, L. Capes, O. Cador, and O. Kahn, J. Am. Chem. Soc. **121**, 10630 (1999).
(22) (a) C. Roux, J. Zarembowitch, B. Gallois, and M. Bolte, New J. Chem. 16, 671 (1992). (b) C. Roux, J. Zarembowitch, B. Gallois, T. Granier, and R. Claude, Inorg. Chem. **33**, 2273 (1994). (c) M.-L. Boillot, C. Roux, J.-P. Audiére, A. Dausse, and J. Zarembowitch, Inorg. Chem. **35**, 3975 (1996).
(23) S. Schenker and A. Hauser, J. Am. Chem. Soc. **116**, 5497 (1994).
(24) S. Schenker, A. Hauser, and R. M. Dyson, Inorg. Chem. **35**, 4676 (1996).
(25) M. A. Berkgamp, P. Gütlich, T. L. Netzel, and N. J. Sutin, J. Phys. Chem. **87**, 3877 (1983).
(26) I. Lawthers and J. J. Mcgarvey, J. Am. Chem. Soc. **106**, 4280 (1984).
(27) S. Hayami, K. Inoue, S. Osaki, and Y. Maeda, Chem. Lett. 987 (1998).
(28) S. Hayami, Y. Hosokoshi, K. Inoue, Y. Einaga, O. Sato, and Y. Maeda, Bull. Chem. Soc. Jpn. **74**, 2361 (2001).
(29) (a) N. Matsumoto, S. Ohta, C. Yoshimura, A. Ohyoshi, S. Kohata, H. Okawa, and Y. Maeda, J. Chem. Soc. Dalton Trans. 2575 (1985). (b) S. Ohta, C. Yoshimura, N. Matsumoto, H. Okawa, and A. Ohyoshi, Bull. Chem. Soc. Jpn. **59**, 155 (1986).
(30) Y. Maeda, H. Ohshio, and Y. Takashima, Chem. Lett. **943** (1982).
(31) S. Schenker, A. Hauser, and R. M. Dyson, Inorg. Chem. **35**, 4676 (1996).
(32) J. A. Real, E. Andrés, M. C. Muñoz, M. Julve, T. Granier, A. Bousseksou, and F. Varret, Science **268**, 265 (1995).
(33) C.-L. Xie and D. N. Hendrickson, J. Am. Chem. Soc. **109**, 6981 (1987).
(34) A. J. Conti, C.-L. Xie, and D. N. Hendrickson, J. Am. Chem. Soc. **111**, 1171 (1989).
(35) A. Hauser, J. Adler, and P. Gütlich, Chem. Phys. Lett. **152**, 468 (1988).
(36) H. Oshio, K. Kitazaki, J. Mishiro, N. Kato, Y. Maeda, and Y. Takashima, J. Chem. Soc. Dalton Trans. 1341 (1987).
(37) S. Hayami and Y. Maeda, Inorg. Chim. Acta **255**, 181 (1997).
(38) G. Ritter, E. König, W. Irler, and H. A. Goodwin, Inorg. Chem. **17**, 224 (1978).
(39) S. M. Nelson, P. D. A. Mcllroy, C. S. Stevenson, E. König, G. Ritter, and J. Waigel, J. Chem. Soc. Dalton Trans. 991 (1986).
(40) S. Hayami, Z.-Z. Gu, M. Shiro, Y. Einaga, A. Fujishima, and O. Sato, J. Am. Chem. Soc. **122**, 7126 (2000).
(41) Y. Garcia, P. J. V. Koningsbruggen, E. Codjovi, R. Lapouyade, O. Kahn, and L. Rabardel, J. Mater. Chem. **7**, 857 (1997).
(42) Y. Garcia, P. J. Koningsbruggen, R. Lapouyade, L. Fournès, L. Rabardel, O. Kahn, V. Ksenofontov, G. Levchenko, and P. Gütlich, Chem. Mater. **10**, 2426 (1998).
(43) H. Köppen, E. W. Müller, C. P. Köhler, H. Spiering, E. Meissner, and P. Gütlich, Chem. Phys. Lett. **91**, 348 (1982).
(44) J. A. Real, H. Bolvin, A. Bousseksou, A. Dworkin, O. Kahn, F. Varret, and J. Zarembowitch, J. Am. Chem. Soc. **114**, 4650 (1992).
(45) R. Jacobi, H. Spiering, and P. Gütlich, J. Phys. Chem. Solids **53**, 267 (1992).
(46) D. Boinnard, A. Bousseksou, A. Dworkin, J.-M. Savariault, F. Varret, and J.-P. Tuchagues, Inorg. Chem. **33**, 271 (1994).
(47) T. Buchen, D. Schollmeyer, and P. Gütlich, Inorg. Chem. **35**, 155 (1996).
(48) J. A. Real, I. Castro, A. Bousseksou, M. Verdaguer, R. Burriel, J. Linares, and F. Varret, Inorg. Chem. **36**, 455 (1997).
(49) H. Spiering, T. Kohlhaas, H. Romstedt, A. Hauser, C. Bruns-Yilmaz, J. Kusz, and P. Gütlich, Coord. Chem. Rev. **190-192**, 629 (1999).
(50) A. J. Simaan, M.-L. Boillot, E. Rivière, A. Boussac, and J.-J. Girerd, Angew. Chem. Int. Ed. **39**, 196 (2000).
(51) J.-F. Létard, P. Guionneau, E. Codjovi, O. Lavastre, G. Bravic, D. Chasseau, and O. Kahn, J. Am. Chem. Soc. **119**, 10861 (1997).
(52) Z. J. Zhong, J. Q. Tao, Z. Yu, C. Y. Dun, Y. J. Liu, and X. Z. You, J. Chem. Soc. Dalton Trans. 327 (1998).
(53) J. Kröber, E. Codjovi, O. Kahn, F. Grolière, and C. Jay, J. Am. Chem. Soc. **115**, 9810 (1993).
(54) J. Kröber, J.-P. Audière, R. Claude, E. Codjovi, O. Kahn, J. G. Haasnoot, F. Grolière, and C. Jay, Chem. Mater. **6**, 1404 (1994).
(55) P. J. V. Koningsbruggen, Y. Garcia, E. Codjovi, R. Lapouyade, O. Kahn, L. Fournès, and L. Rabardel, J. Mater. Chem. **7**, 2069 (1997).
(56) M. Sorai, J. Ensling, and P. Gütlich, Chem. Phys. **18**, 199 (1976).
(57) M. Sorai, J. Ensling, K. M. Hasselbach, and P. Gütlich, Chem. Phys. **20**, 197 (1977).
(58) S. Hayami, Z.-Z Gu, H. Yoshiki, A. Fujishima, and O. Sato, J. Am. Chem. Soc. **123**, 11644 (2001).